Triple Pulse Test (TPT) for Characterizing Power Loss in Magnetic Components in Analogous to Double Pulse Test (DPT) for Power Electronics Devices

Jun Wang, Xibo Yuan, Navid Rasekh
Department of Electrical and Electronic Engineering, University of Bristol
Bristol, United Kingdom
Email: jun.wang@bristol.ac.uk; xibo.yuan@bristol.ac.uk; navid.rasekh@bristol.ac.uk

***Abstract*—Power loss modelling of magnetic components becomes increasingly important in the design of modern power electronic converters, especially in the case of higher switching frequencies enabled by emerging wide-bandgap devices. While the modelling of the active power electronic devices is relatively mature and straightforward, the estimation of the passive magnetic component loss remains challenging, including both the core loss and winding (copper) loss. As indicated by recent studies, the accurate prediction of the core loss in power converters relies on rectangular-voltage-excited measurements. To characterize the core loss with high-frequency rectangular excitations and dc-biases, a Triple Pulse Test (TPT) has been proposed and is further extended in this paper. The TPT involves a discontinuous procedure and a bidirectional, half-bridge excitation circuit that supplies transitional high rectangular voltage and high current. The importance and practical considerations of achieving closed dynamic BH loops are discussed. The proposed TPT is analogous to the common Double Pulse Test (DPT) for power electronics devices in terms of the testing circuit, the measurement instruments, and the discontinuous procedure. Moreover, the winding loss characterization can also be achieved by the TPT, given the winding loss can be very difficult to predict especially for randomly wound components where analytical equations cannot be applied accurately. Eventually, a complete loss dataset for one magnetic component design (i.e. same core material, shape and winding arrangement) can be built from TPT, which can be utilized to accurately model the inductor loss in power converter applications.**

Keywords—triple pulse test, double pulse test, core loss, BH loop measurement, copper loss

I. INTRODUCTION

Along with the development of high-switching-frequency power converters, the loss modelling of the active and passive components become increasingly important in order to achieve reliable thermal design and reduce the prototyping cycles. The modelling and characterization of the power electronics devices, such as IGBTs and MOSFETs, are relatively mature and accurate, which includes the conduction loss and the switching loss. In practice, the conduction loss and switching loss of power devices are characterized experimentally by the manufacturers, for which the results are widely supplied to the users in the manufactuerer datasheets. While the conduction loss can be simply modeled as an on-state resistance, e.g. $R_{ds(ON)}$ for MOSFETs, the switching loss is commonly modeled in the form of the loss energy of one switching transition in relation to the switching voltage and current, which is characterized through the Double Pulse Test (DPT) [1] against various configurations and operating points. The tested dataset enables the users to estimate the switching loss for real operating conditions (switching voltage and current) without reproducing the detailed transitional voltage and current waveforms.

The loss modelling of magnetic components is more challenging, in which the core loss is the major challenge. Because of the non-linear nature, the core loss cannot be modelled fully by physical models. The only practical approach to estimate the core loss is based on empirically measured dataset [2], [3], which in principle is similar to the switching loss dataset for power electronics devices. Given the pre-produced core loss data, the instantaneous magnetization and demagnetization process of the magnetic cores do not need to be modelled to predict the power loss occurred. Currently, the common practice of the manufacturers is to provide a core loss datasheet for one particular type of magnetic material, which is measured from sinusoidal excitations. As the widely accepted approach, the provided datasheet is then converted to Steinmetz Equation (SE) parameters as follows for the loss prediction purpose in sinusoidal-excited applications, e.g. electric machines

$$P = kf^{\alpha}\Delta B^{\beta} \tag{1}$$

However, for power electronics applications with rectangular excitations, the core loss prediction is less straightforward. Academia and industry have not reached a consensus on a generally applicable approach in this case. The conventional approaches based on Steinmetz Equations and its variations, e.g. improved generalized Steinmetz equations (iGSE), cannot accurately account for the rectangular excitation with dc-biased current and a harmonic spectrum crossing a wide range of frequencies [2], [4]. The frequency dependency of the SE parameters [2] indicates that the SE is not a perfect curve-fitting expression for the non-linear core loss phenomenon.

As a recent advance, academics have proposed to collect the core loss data directly from rectangular excitations for better accuracy of estimation [4]–[7]. The rectangular-excitation-based dataset can be straightforwardly utilized in predicting the core loss of filter inductors in pulse width modulated (PWM)

converters as presented in [6]–[9]. Implementing rectangular excitation voltage to build the core loss dataset can be seen as emulating the actual waveforms, that an inductor will experience in a power converter, in a standalone test setup.

In terms of the winding loss of magnetic components, although it can be well predicted by analytical models or finite element analysis (FEA), it still poses challenges in practice where the physical positioning of the wires cannot be accurately modelled, e.g. in a hand-wound inductor with random conductor placement. With the increase of frequency, the proximity effect and skin effect can also be very challenging to model accurately. Therefore, the practical solution could also be to generate a copper loss dataset from empirical testing.

At the time of this work, the manufacturers still do not provide the inductor loss data measured from rectangular excitations. Moreover, the available manufacturer datasheets of core loss are typically for per magnetic material only, rather than per inductor/transformer. In contrast, each power electronics device, e.g. one packaged IGBT or MOSFET, commonly has its individual switching loss data in the datasheet, instead of just the properties of the semiconductor material. As demonstrated in [7], if the core loss data is generated for each inductor/transformer design (i.e. same core material, shape and winding arrangement), it will be more accurate and more user-friendly for power electronics applications. If the empirical testing is performed on one inductor/transformer design, the copper loss can also be included as the windings are fixed. To test one built inductor/transformer design, it may require a high-voltage/current excitation circuit and high-power measurement instruments, while testing one magnetic material normally requires only a low-power test setup.

This paper proposes and demonstrates a triple pulse test (TPT) that involves a discontinuous testing procedure and a high-voltage/current, rectangular excitation circuit. Due to the discontinuous feature, the TPT procedure simplifies the testing process and requires only a transient power capability of the test setup. While the TPT concept has been brought up in a previous publication [7], this work demonstrates supplementary practical considerations of the testing and, more importantly, further extends its concept to include the copper loss to form a complete loss dataset of a magnetic component. Additionally, a detailed comparison between the Triple Pulse Test and the Double Pulse Test is demonstrated in this work to show their resemblance in terms of concept and practicability for better understanding by the audiences, e.g. power electronics engineers. An experimental case study is then conducted on one built inductor in a test rig.

II. Triple Pulse Test for Core Loss under Rectangular Excitation Voltage

A. Two-winding dynamic B-H loop measurement

To measure the loss of magnetic components, there are mainly two practical approaches: (1) thermal-based approach such as calorimetric method and graphic method [10] (2) electrical-based approach, i.e. the two-winding method. The two-winding dynamic B-H loop measurement has been widely applied in characterizing the high-frequency core loss of a magnetic component/material [6], [11]. Compared to the thermal based method, the two-winding method has the following benefits:

- Include only the core loss, i.e. the hysteresis loss, eddy current loss and residual loss, and exclude the copper loss. By using the secondary sensing winding, the voltage drops owing to the resistance of the primary winding and leakage inductance are not included in the measurement [11].
- Ability to capture the core loss in a very short transition, e.g. a switching cycle of in high-frequency power converters, without the need to achieve thermal steady state. The transitional core loss is captured in the form of a dynamic B-H loop [6].

Fig. 1 shows a top-level illustration of the B-H loop measurement, which is formed by a power converter, the magnetic device for testing and the measurement instruments.

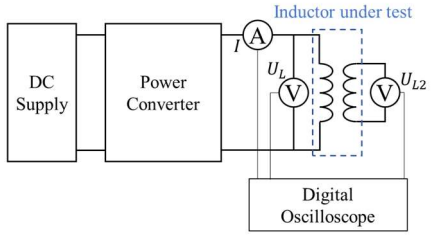

Fig. 1. B-H loop measurement setup.

The magnetic-domain operation of the magnetic core is found in the form of the trajectory in the plane of flux density B and the magnetic field H. The B and H are captured from the electrically measured waveforms, i.e. the excitation current I and the open-circuit voltage on a sensing coil U_{L2}, as expressed in (2) and (3).

$$H(t) = \frac{N_1 \cdot I(t)}{l_e} \tag{2}$$

$$B(t) = \frac{1}{N_2 A_e} \int_0^t U_{L2}(t)\, dt \;\; (B(0) = 0) \tag{3}$$

where N_1 is the number of turns of the main winding of the inductor; N_2 is the number of turns of the flux-sensing winding; A_e is the effective cross-section area of the core; l_e is the effective length of magnetic path of the core.

When the BH trajectory forms a closed loop over a period of $2T$, the core loss occurred in this process is expressed as

$$E_{core} = A_e l_e \int H\, dB = \frac{N_1}{N_2} \int_0^{2T} I(t) \cdot U_{L2}(t)\, dt \tag{4}$$

Note that the measured dynamic BH trajectory should ideally form a closed loop. If the measured BH loop is unclosed, it indicates that the magnetization/demagnetization process is not fully completed, which results in reactive energy unreturned from the core that will be incorrectly accounted as the loss in (4). This case is also elaborated in [6], where an open-looped

trajectory leads to excessive loss incorrectly included for a high-frequency dynamic loop.

Additionally, the existing core loss calculation methods for PWM converters relies on an important assumption – the magnetization (positive) cycle and the demagnetization (negative) cycle equally consumes half of the total loss in the whole loop. This assumption enables the PWM waveforms to be decomposed into pulse segments for the core loss calculation as implemented in [4], [7], [8]. This assumption only stands in the case of a closed and symmetric BH loop.

B. Excitation circuit

This section discusses the excitation circuit for the rectangular-excited BH loop measurement. As introduced, to form a dataset that can be later used for estimating the core loss in power converters, it is intended to emulate the same operations of the core in a standalone BH loop measurement. To accurately emulate the operations in a PWM converter, the typical inductor waveform shown in Fig. 2 must be considered.

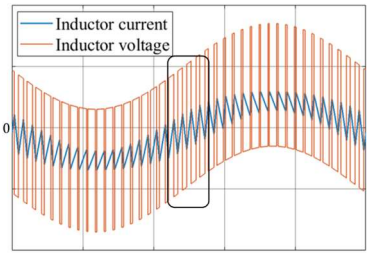

Fig. 2. Typical voltage/current waveform of a filter inductor in a two-level dc/ac PWM converter.

As shown in the figure, on switching cycle basis, the inductor experiences quasi-rectangular excitations with various amplitudes, duty cycles and dc-biased current. If the device-under-test is a high-power inductor, the excitation circuit needs to have the ability to emulate the high voltage and high current as in a real high-power converter application.

Note in some switching cycles marked in Fig. 2, the current is bidirectional, which passes through the positive and negative region. This case happens when the dc-bias current is small while the current ripple amplitude is large. Therefore, ideally, the excitation circuit for the BH loop measurement should be bidirectional to account for these switching cycles with bidirectional current flows.

In previous studies [6], [8], a dc chopper (buck) circuit has been utilized as the excitation circuit for the BH loop measurement, which is the simplest solution for testing dc-biased operating points. However, this excitation circuit is unidirectional and cannot cover the operating points with bidirectional current flows. If these cases are not evaluated, the subsequent core loss dataset would be incomplete for the estimation purpose.

There are two solutions to achieve the target high-voltage/current bidirectional excitation. Firstly, as the most common solution of a single-phase dc/ac converter, a full bridge can be used for the testing as implemented in [12], [13]. However, the most significant flaw of this configuration is the significant device voltage drops causing the asymmetric rectangular voltage on the inductor under a high dc-bias current, as pointed out in [7]. An asymmetric rectangular voltage will lead to unclosed BH loops as a result of unequal volt-second product applied on the inductor in the positive cycle and the negative cycle respectively.

To overcome this limitation, a half-bridge excitation circuit with two dc sources is proposed by us in [7], which is presented in Fig. 3. Although this half-bridge configuration has been implemented ealier in [14], it did not have two dc courses in series. Fig. 3 shows the case where the target dynamic BH loop is "floating" in the first quadrant of the BH plane due to the dc-biased current, which is the major case in the intended testing. In this case, the inductor current is always positive so that only switch T1 needs to operate.

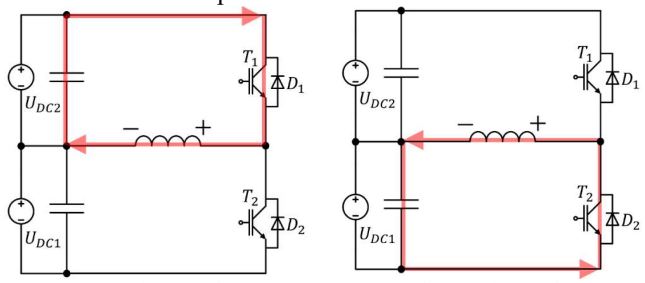

Fig. 3. Proposed half-bridge test circuit with dc-biased current

The inductor voltage in the positive cycle and the negative cycle in this circuit is expressed as follows considering the device voltage drops

$$U_{L+} = U_{DC2} - U_{IGBT} \quad (5)$$

$$U_{L-} = -(U_{DC1} + U_{Diode}) \quad (6)$$

Under a high dc-biased current, if the two dc capacitor voltages are equal and not adjustable, there will be a difference between U_{L+} and $|U_{L-}|$. Note this asymmetric is caused not only by unequal U_{Diode} and U_{IGBT}, but also the plus/minus sign in (5) and (6). For example, if U_{DC2}= U_{DC1} = 50V, U_{IGBT} = 3 V and U_{Diode} = 2 V, the inductor-under-test will experience a rectangular voltage with +47V in the positive cycle and -52 V in the negative cycle. By adjusting the two separate dc source voltages (U_{DC2} and U_{DC1}), it can compensate the asymmetric rectangular voltage amplitudes due to the device voltage drops under a dc-biased current. This degree of freedom does not exist in the full-bridge configuration or the regular half-bridge configuration. Note when the target current is bidirectional, both T1 and T4 need to operate and the asymmetric of voltage amplitude will not be a concern due to the complementary conduction path.

C. Triple pulse test procedure

Based on the proposed testing circuit, a TPT procedure is proposed as follows with the testing waveforms illustrated in Fig. 4. The amplitude of the testing is fixed to half the dc-link voltage. To build up a dc-bias current, an initial wide gate pulse is applied to turn on T1, which is referred as the 1st pulse. Next, as the second stage, narrower pulses with the target width (T= t_2 = t_{2+} = t_{2-}) are applied, which is referred as the 2nd pulse or pulses. These cycles intend to drive the inductor into an

electrical/magnetic steady state operating at the target high-frequency dynamic loop. Once the waveforms are stabilized, it enters the third stage, where one target full cycle of the dynamic loop is captured. This captured cycle should form a closed BH loop that features a certain dc-biased current (pre-magnetization), volt-second product (flux density swing) and voltage amplitude (*dB/dt*). After the third stage, T1 is turned off and the current freewheels in the diode D2 to release the energy stored in the inductor until it is fully discharged. The whole process last for a period of typically 100 ~ 500 μs. This discontinuous concept and testing waveform are similar to the approach used in the saturation property test in [15].

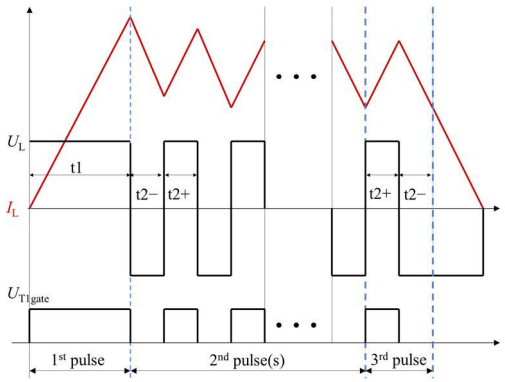

Fig. 4. Illustration of the testing waveforms of the TPT with a dc-bias current

The width of the first pulse t_1 is calculated from the target dc-bias current, the voltage amplitude and the inductance of the component (which is assumed to be the nominal value) as

$$t_1 = I_0 \cdot L/U_L + 0.5 \cdot t_2 \tag{7}$$

This TPT procedure is discontinuous as it intends to capture the first steady-state dynamic BH loop and avoid unnecessary further operations. If the excitation were continued, the BH trajectory would only repeat the target dynamic loop because it already reached the steady state. Therefore, the proposed TPT procedure should lead to the same results as regular approaches where the excitation is continuous. This discontinuous capturing technique is implemented through the digital oscilloscope and post-processing software such as Matlab. To reduce the effect of random noise, the same procedure can be repeated, and the averaged trajectory of the target BH loop can be obtained from repeated runs, e.g. 20 runs. The proposed discontinuous procedure has the following merits:

a) The testing setup does not require the full continuous power capacity. The transitional high dc-biased current (e.g. >100A) is drawn from the dc-link capacitors rather than the dc power supplies, which will not trigger the current protection of the dc sources. In the case of measuring the current with a current probe, this procedure avoids a large dc current-time product that is limited by the design of the current probes.

b) Because of the short testing transition, very small amount of heat will be generated, which can be neglected. Therefore, this testing does not vary the temperature of the component-under-test. Additionally, it does not need a full-scale cooling heatsink to process the heat generated in the testing. For example, if the inductor is designed for high-power operations accompanied with a liquid cooling system, it does not require the full-scale cooling system in the discontinuous TPT setup.

D. Summary and practical considerations

A triple pulse test procedure is introduced in this section, which involves a half-bridge excitation circuit and a discontinuous procedure. Note in existing approaches, the alternative to establish the dc-bias current is to apply a separate dc current source through a third bias winding [16]. In contrast, the proposed TPT procedure does not require extra hardware while the dc-biased current is established through adjusting the width of the first pulse.

As discussed, forming a closed dynamic BH loop is important to achieve an accurate capturing of the core loss over a target cycle. An unclosed dynamic BH loop leads to incorrectly captured core loss that does not belong to the target dynamic cycle, which compromises the critical assumption that the magnetizing and demagnetizing cycles each consumes half of the core loss of the loop. In practical TPT, there are following aspects that need to be considered to achieve a closed BH loop:

- The rectangular excitation voltage in the positive and negative cycles should be symmetric which features:
  - Equal voltage amplitudes
  - Equal volt-second product
- The operation of inductor core should enter the steady state
- The phase discrepancy and dc offset of the probes should be compensated

To achieve the symmetric rectangular excitation should be ensured, the presented half-bridge excitation circuit provides the ability to compensate the unequal amplitudes due to device voltage drops by adjusting the two dc-link capacitor voltages, as demonstrated in Section II.B. Apart from the equal voltage amplitudes, the pulse widths of the positive/negative cycles also need to be calibrated to prevent unequal volt-second product and subsequently to avoid unclosed B-H loop. If the power devices in the excitation circuit are IGBTs, the turn-on and turn-off transitions last unequal duration. For example, for power module SKiM301TMLI12E4B, the turn-on time is 218 ns and the turn-off time is 355 ns due to the tail current. This unequal switching time will lead to unequal volt-second product on the inductor in the positive and negative cycles, which will result in unclosed BH loop in the testing. This non-ideal operation can be compensated in the generation of gate signals through a fine adjustment of the pulse widths. For example, considering a longer turn-off transition of IGBTs, the width of the positive cycle t_{2+} should be reduced in practice.

Apart from the symmetricity of the excitation voltage, the operation of the inductor core should enter the steady state to achieve a closed target BH loop, as intended in the TPT concept. This objective can be realized by adjusting the number of stabilizing pulses on case to case basis.

From the measurement point of view, the phase discrepancy between the voltage and current probes in the testing will significantly affect the accuracy of the core loss measurement

[3]. The reason is that the pair of voltage and current used to obtain the core loss energy in (4) has a phase difference of close to 90°, because the operation of the inductor/transformer is mainly reactive. The error in the phase discrepancy will incorrectly count the energy absorbed and returned from the reactive cores, and lead to incorrect consumed loss captured in (4). To address this issue, the phase discrepancy needs to be carefully calibrated, e.g. through a de-skew tool and the de-skew function on the oscilloscope. Alternatively, the reactive voltage cancellation concepts [17], [18] have been proposed in recent years which add an additional resonance capacitor or reference transformer in the testing circuit, so that the voltage/current pair under integration in (4) will be in phase. In short, the phase discrepancy issue lies in the measurement and load circuit of the testing. The excitation circuit and the procedure in the proposed TPT is still applicable in the reactive voltage cancellation circuits.

In practice, even though the above measures are all implemented, the target B-H loop may still not completely close due to uncontrollable non-ideal factors in the test rig (e.g. ringing in the voltage due to circuit parasitics). In this case, the BH loop can be virtually closed by connecting the start and end point in the data post-processing to minimize the effect of unreturned reactive energy shown as unclosed BH loop.

III. Analogy between DPT and TPT

For better understanding by the audiences, this section elaborates the resemblance between DPT and TPT from the following aspects in terms of both concept and practical implementation:

- High-voltage/current testing circuit and instruments
- Discontinuous concept with the first pulse to build up the dc-bias current
- Format of the generated dataset

Firstly, the testing circuits of both TPT and DPT are based on a half-bridge topology. Illustrations of both testing circuits are shown in Fig. 5. The power devices are in the same configuration in both circuits, which can be a half-bridge power module for instance. When the inductor is tested with a dc-bias current, only switch T1 is controlled by the triple gate pulses as shown in Fig. 5(a), which is similar to the DPT in Fig. 5(b) where the IGBT/MOSFET under test is fed with double gate pulses. Both testing circuits desire a large dc-link capacitance, because ideally the dc-link voltage needs to stay relatively constant (e.g. the voltage deviation stays below 1%) over the whole testing window while the transitional current/energy in is drawn from these capacitors. The main difference in the TPT is the two dc sources required for the voltage drop compensation purpose. In terms of the testing instruments, both setups require high-bandwidth current and voltage probes to capture the detailed transitional voltage/current waveforms. In both cases, the waveforms are captured in digital oscilloscopes and post-processed by computer software, such as Matlab.

Secondly, both testing procedures share the discontinuous concept. The typical testing waveforms are illustrated in Fig. 6.

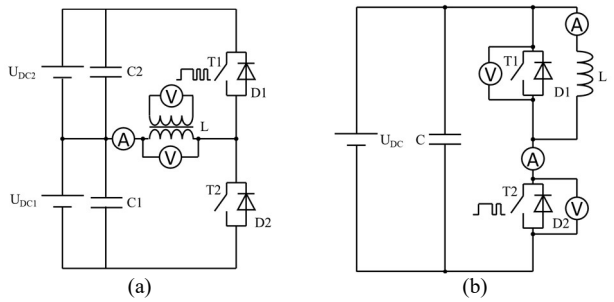

Fig. 5. Illustration of testing circuit (a) TPT for inductor core loss with dc-bias (b) DPT for switching loss of T2/D1

The discontinuous procedure reaches the target window of interest with minimized process and avoids unnecessary operation. As discussed in Section II.A, the discontinuous concept is beneficial mainly because it reduces the power requirement of the testing setup and avoids temperature variation due to the little heat generated in the short transition. The typical window of the captured waveform of DPT is at the level of 100 ns, which focuses on the turn-on/turn-off edges. For the TPT, the captured window of a TPT is typically at 10 ~ 200 µs for example, which covers one full cycle of the rectangular excitation, e.g. 5 kHz ~ 100 kHz. Additionally, both testing procedures utilize the first pulse to establish a dc-bias current. The purpose of it is to emulate the switching current of the power device in the DPT and to emulate the dc-biased pre-magnetization of the magnetic core in the TPT.

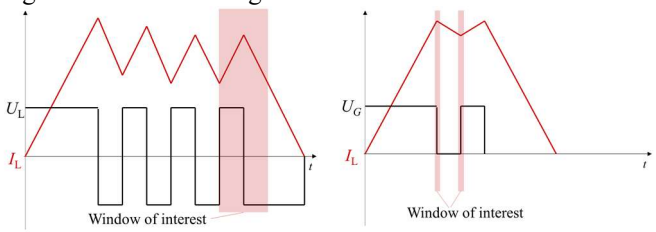

Fig. 6. Illustration of typical testing waveforms (inductor current I_L; inductor voltage U_L; device gate voltage U_G)

Thirdly, in terms of the outcome of the testing, TPT and DPT also lead to similar form of the generated dataset. DPT results in the loss energy of one switching transition that is described by three variables as following, regardless of the temperature

$$E_{sw}(mJ) = f(R_G, U_{sw}, I_{sw}) \tag{8}$$

where U_{sw} is the switching voltage, I_{sw} is the switching current and R_G is the gate resistance.

For the magnetic components, the core loss under rectangular excitation is also expressed in a three-dimensional dataset as follows regardless of the temperature [6]

$$E_{core}(mJ) = g(\Delta B, \frac{dB}{dt}, H_0) \tag{9}$$

where E_{core} is the core loss energy of one closed BH loop; ΔB is the flux density swing; dB/dt is the change rate of the flux density and H_0 is the dc-bias of the magnetic field.

When it comes to one inductor design, due to the fixed core geometries, the three variables above can be converted to the

primary-side electrical variables to form the "user-friendly core loss map" [7] as

$$E_{core}(mJ) = h(U_L \cdot T, U_L, I_0) \quad (10)$$

where E_{core} is the core loss energy of one pulse; U_L is the main inductor winding voltage amplitude measured in Fig. 1, T is the period of one pulse (half of a symmetric BH loop), I_0 is the biased current.

In short, regarding the form of the empirically generated dataset, the switching loss data from DPT and the core loss data from TPT are both defined by three operational variables.

IV. TPT FOR COPPER LOSS AND TOTAL INDUCTOR LOSS

A. Measurement of copper loss and total inductor loss in TPT

The presented TPT is able to account for not only the core loss, but also the copper loss. By replacing the secondary voltage U_{L2} in (4) with the main winding voltage U_L in Fig. 1 as below, the total inductor loss can be obtained for one BH loop segment, which is also brought up in [17], [18]

$$Q = \int_0^T I(t) \cdot U_L(t)\, dt \quad (11)$$

The difference between the measured total inductor loss and the core loss is the copper loss. Fig. 7 shows an experimental example of the integration of the instantaneous power over the primary/second voltage and the current in a target cycle. Over one full cycle, the end point of the red trajectory indicates the total inductor loss occurred in this cycle, which is 1.397 mJ in this case, while the blue trajectory indicates the core loss, which is 1.174 mJ in this case. Therefore, the difference in between these two loss values is the copper loss, which is 0.223 mJ in this case. This example demonstrates that both the copper loss and core loss can be captured in the TPT for one cycle of rectangular excitation.

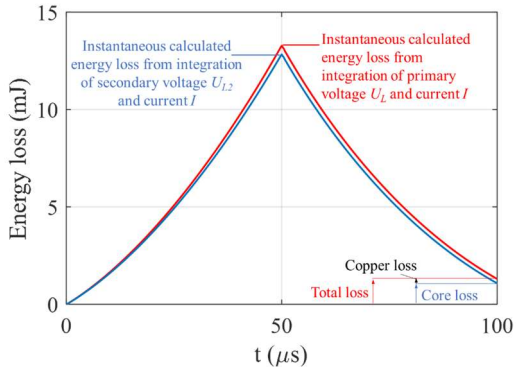

Fig. 7. Integration of instantaneous power over a target cycle captured in experiment (corresponds to the target cycle in Fig. 10 in Section V)

B. User-friendly total loss dataset for one inductor design

Because the total inductor loss can be captured in the TPT, this work proposes that a user-friendly total loss dataset should be produced to the users for each inductor design based on empirical measurements through TPT. Ideally, the inductor/transformer loss dataset should be measured by the manufacturers, so that the users can utilize these data directly in modeling the power loss of magnetic components in power electronics. This is a similar concept as the switching loss datasheet supplied by the manufacturers of IGBTs/MOSFETs.

As introduced, one operating cycle of an inductor core can be described by three variables: $U_L{\cdot}T$, U_L and I_0. The copper loss dataset can also be expressed by the same three variables. With reference to the conventional copper loss models, the variable I_0 reflects the dc copper loss. The other two variables, $U_L \cdot T$ and U_L represent a unique rectangular excitation pattern and a unique triangular current waveform in an inductor, which reflects the ac copper loss.

In short, the copper loss and the total loss of an inductor/transformer design can also be expressed by the three variables in a user-friendly loss map, i.e. $U_L \cdot T$, U_L and I_0. Once this three-dimensional loss dataset is provided by the manufacturer, the users can model the inductor loss by modelling the ideal inductor voltage/current waveforms. In this way, the prediction of the dynamic non-ideal effects is avoided, e.g. the distorted curvy shape of the inductor current [6], [7] caused by the non-linear core magnetization process.

For practical purposes, the proposed inductor loss map is implemented as a multi-dimensional lookup table as illustrated in Fig. 8, where the core loss, copper loss and total loss can be found through the three indexing variables.

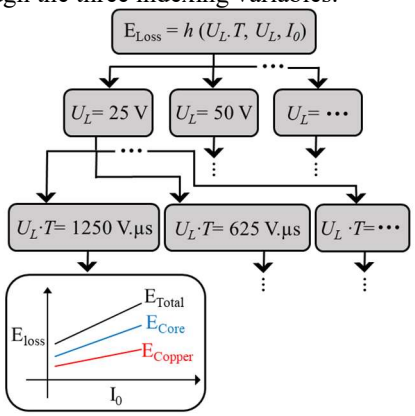

Fig. 8. Illustration of the proposed multi-dimensional inductor loss map

V. EXPERIMENTAL RESULTS

An experimental test rig has been built to perform the proposed TPT. A picture of the test rig is shown in Fig. 9. The components and instruments in the test rig are listed in Table I.

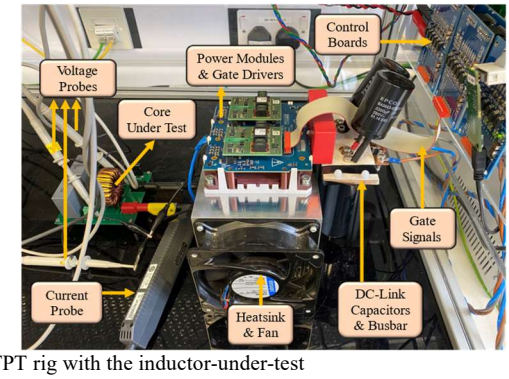

Fig. 9. TPT rig with the inductor-under-test

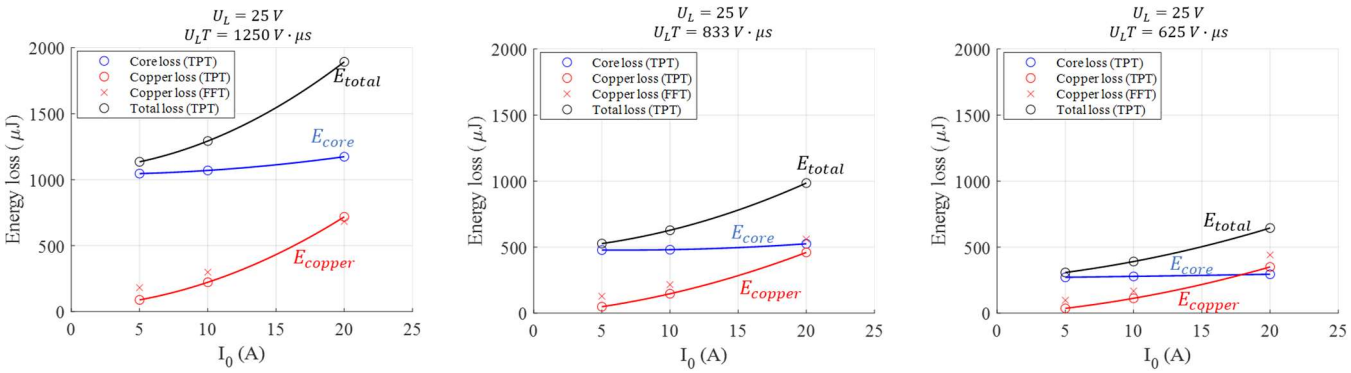

(a) $U_L \cdot T$ = 1250 V·µs (b) $U_L \cdot T$ = 833 V·µs (c) $U_L \cdot T$ = 625 V·µs

Fig. 12. Inductor loss maps generated from experimental triple pulse tests (U_L = 25V)

TABLE I COMPONENTS AND INSTRUMENTS IN THE TEST RIG

Power supplies	Elektro-Automatik TS 8000 T
Voltage probe	Keysight N2862B (150 MHz)
Current probe	Keysight N2783B (100 MHz)
Power module	Semikron SKiM301TMLI12E4B
Tested inductor	92 µH, T184-26 from Micrometals©, *N*1:*N*2 = 24:24
Digital oscilloscope	MSO-X 3054A (500 MHz, 4 GSa/s)

Fig. 10 shows an example of the test waveform of one operating point of the inductor-under-test.

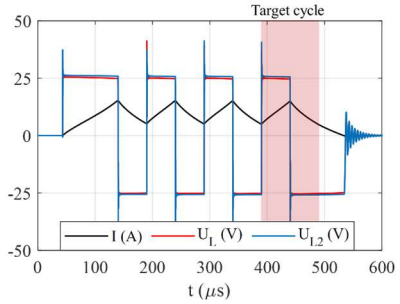

Fig. 10. Experimental current/voltage waveform of one TPT test (U_L = 25 V, I_0 = 10 A, T = 50 µs)

In this tested point, a dc-bias current is established in the first pulse, which is followed by two pulse cycles to stabilize. The target cycle is achieved in the final pulse cycle with a dc biased current of 10 A and an equivalent 10 kHz square-wave excitation voltage with 25 V amplitude.

Converted from the measured waveforms in Fig. 10, the BH trajectory of the whole TPT process is plotted in Fig. 11. It can be seen that a closed BH loop is achieved in the target cycle after two stabilizing cycles. The core loss measured in this closed BH loop is 1.174 mJ.

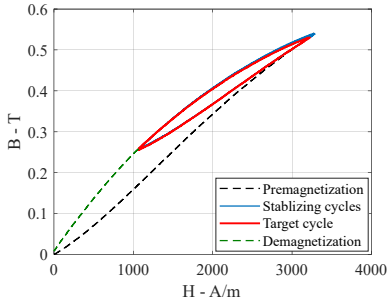

Fig. 11. Experimental BH trajectory of one TPT test run. ΔB = 280 mT (U_LT = 1250 V·µs); dB/dt = 5600 T/s (U_L = 25 V); H_0 = 2200 A/m (I_0 = 10 A).

By repeating the TPT for various operating point, Fig. 12 shows the inductor loss maps generated from experimental testing, which shows the copper loss, core loss and total inductor loss. The discrete results are fitted with a second order approximation. These loss graphs are expected to be included in future manufacturer datasheets as illustrated in Fig. 8. These empirical loss maps can then be utilized to accurately model the inductor loss for PWM converters once the inductor operating space (described by $U_L \cdot T$, U_L and I_0) are identified on switching cycle basis, e.g. through analytical models presented in [9] or through simulation and experiments.

To validate the copper loss measured from TPT, the copper loss is also estimated by performing Fast Fourier Transformation (FFT) and calculating the copper loss [19] as

$$P_w = R_{wdc} I_{dc}^2 + \sum_{n=1}^{\infty} R_{wacn} I_n^2 \qquad (12)$$

where the dc winding resistance R_{wdc} and the ac winding resistance R_{wacn} across the frequency spectrum are measured by impedance analyzer Wayne Kerr 6500B; The dc current component I_{dc} and the ac current component I_n across the frequency spectrum are extracted from the measured current of the target segment through FFT. The copper loss results estimated by FFT are shown in Fig. 12 as red cross markers, which show consistency with the TPT measured results. Given that the accuracy of TPT in capturing the core loss has been verified in [7], the above results validate the proposed approach in capturing the copper loss and total inductor loss through TPT.

VI. CONCLUSION

This work has proposed and elaborated a Triple Pulse Test (TPT) for characterizing the magnetic component losses. The TPT intends to emulate the operation of an inductor/transformer in a standalone test setup, where the core loss is captured in the form of the energy loss of a dynamic BH loop. The TPT involves a high-voltage/current bidirectional excitation circuit and a discontinuous testing procedure. Because the discontinuous procedure only involves several short pulses, the need of a continuous high-power test setup is avoided. To accurately extract the core loss in practice, the realized dynamic BH loops should ideally form closed loops. Practical efforts to achieve the closed BH loops are elaborated in this work, including the compensation of unequal voltage amplitudes due

to device voltage drops and the compensation of asymmetric rising/falling edge due to the unequal device turn-on/turn-off time.

The concept of the proposed TPT is analogous to the well-known Double Pulse Test (DPT) for power electronics devices (e.g. IGBTs and MOSFETs), in terms of the testing circuit, the measurement instrument, the discontinuous procedure and the format of generated power loss dataset. The similarity between the DPT and TPT is helpful for the power electronics engineers/researchers to comprehend and implement in practice.

This work also extends the TPT to include the copper loss so that the total inductor loss is characterized in the procedure, considering that the analytical modelling of copper loss can also be challenging in practice due to complex positioning of the windings and high-frequency effects. With fixed winding and core shapes, the TPT can be performed on one inductor design to build an empirical data pool of the inductor losses indexed by three variables. Considering that there are more and more standardized inductors manufactured nowadays, it can be anticipated that the manufacturers would produce the proposed inductor loss map for each inductor design. This pre-produced dataset will enable the users to accurately calculate the magnetic component loss on switching cycle basis in a power converter, without modelling the non-ideal winding positioning or the non-linear magnetization process that cannot be fully expressed by physical models.

ACKNOWLEDGMENT

The authors would like to thank the UK Royal Academy of Engineering for funding part of this work.

REFERENCES

[1] Semikron, "Determining Switching Losses of SEMIKRON IGBT Modules," 2014. [Online]. Available: https://www.semikron.com/dl/service-support/downloads/download/semikron-application-note-switchinglosses-en-2014-08-19-rev-00/.

[2] K. Venkatachalam, C. R. Sullivan, T. Abdallah, and H. Tacca, "Accurate prediction of ferrite core loss with nonsimisoidal waveforms using only steinmetz parameters," in *Proc. IEEE Workshop on Computers in Power Electronics*, 2002, pp. 36–41.

[3] F. D. Tan, J. L. Vollin, and S. M. Cuk, "A practical approach for magnetic core-loss characterization," *IEEE Transactions on Power Electronics*, vol. 10, no. 2, pp. 572–578, Mar. 1995.

[4] C. R. Sullivan and J. H. Harris, "Testing core loss for rectangular waveforms," 2010. [Online]. Available: http://www.psma.com/coreloss/pilot.pdf.

[5] E. Herbert, "Testing core loss for rectangular waveforms, phase II supplemental report," 2012. [Online]. Available: http://www.psma.com/coreloss/supplement.pdf.

[6] T. Shimizu and S. Iyasu, "A practical iron loss calculation for AC filter inductors used in PWM inverters," *IEEE Transactions on Industrial Electronics*, vol. 56, no. 7, pp. 2600–2609, 2009.

[7] J. Wang, K. J. Dagan, X. Yuan, W. Wang, and P. H. Mellor, "A practical approach for core loss estimation of a high-current gapped inductor in PWM converters with a user-friendly loss map," *IEEE Transactions on Power Electronics*, vol. 34, no. 6, pp. 5697–5710, Jun. 2019.

[8] H. Matsumori, T. Shimizu, K. Takano, and H. Ishii, "Evaluation of iron loss of AC filter inductor used in three-phase PWM inverters based on an iron loss analyzer," *IEEE Transactions on Power Electronics*, vol. 31, no. 4, pp. 3080–3095, 2016.

[9] J. Wang, K. J. Dagan, and X. Yuan, "An efficient analytical inductor core loss calculation method for two-level and three-level PWM converters based on a user-friendly loss map," in *IEEE Proc. Applied Power Electronics Conference and Exposition*, 2019.

[10] B. Liu, W. Chen, J. Wang, and Q. Chen, "A practical inductor loss testing scheme and device with high frequency PWM excitations," *IEEE Transactions on Industrial Electronics*, 2020.

[11] V. J. Thottuvelil, T. G. Wilson, and H. A. Owen, "High-frequency measurement techniques for magnetic cores," *IEEE Transactions on Power Electronics*, vol. 5, no. 1, pp. 41–53, 1990.

[12] J. Mühlethaler *et al.*, "Improved Core-Loss Calculation for Magnetic Components Employed in Power Electronic Systems," *IEEE Transactions on Power Electronics*, vol. 27, no. 2, pp. 964–973, 2012.

[13] C. R. Sullivan, J. H. Harris, and E. Herbert, "Core loss predictions for general PWM waveforms from a simplified set of measured data," in *Proc. IEEE Applied Power Electronics Conference and Exposition*, 2010, pp. 1048–1055.

[14] D. Y. Chen, "Comparisons of high frequency magnetic core losses under two different driving conditions: A sinusoidal voltage and a square-wave voltage," in *PESC Record - IEEE Annual Power Electronics Specialists Conference*, 1978.

[15] K. Umetani, "Improvement of saturation property of iron powder core by flux homogenizing structure," *IEEJ Transactions on Electrical and Electronic Engineering*, vol. 8, no. 6, pp. 640–648, 2013.

[16] L. Chang, T. M. Jahns, and R. Blissenbach, "Characterization and Modeling of Soft Magnetic Materials for Improved Estimation of PWM-Induced Iron Loss," *IEEE Transactions on Industry Applications*, vol. 56, no. 1, pp. 287–300, 2020.

[17] D. Hou, M. Mu, F. C. Lee, and Q. Li, "New high-frequency core loss measurement method with partial cancellation concept," *IEEE Transactions on Power Electronics*, vol. 32, no. 4, pp. 2987–2994, 2017.

[18] M. Mu, Q. Li, D. J. Gilham, F. C. Lee, and K. D. T. T. Ngo, "New core loss measurement method for high-frequency magnetic materials," *IEEE Transactions on Power Electronics*, vol. 29, no. 8, pp. 4374–4381, 2014.

[19] K. K. Marian, *High-Frequency Magnetic Components*, 2nd ed. Chichester: WILEY, 2014.